Main-chain organometallic polymers comprising redox-active iron(II) centers connected by ditopic *N*-heterocyclic carbenes†

Laszlo Mercs,[a] Antonia Neels,[b] Helen Stoeckli-Evans[c] and Martin Albrecht*[a,d]

Main-chain organometallic polymers were synthesized from bimetallic iron(II) complexes containing a ditopic *N*-heterocyclic carbene (NHC) ligand [(cp)(CO)LFe(NHC~NHC)Fe(cp)(CO)L]X_2 (where NHC~NHC represents a bridging dicarbene ligand, L = I^- or CO). Addition of a diimine ligand such as pyrazine or 4,4′-bipyridine, interconnected these bimetallic complexes and gave the corresponding co-polymers containing iron centers that are alternately linked by a dicarbene and a diimine ligand. Diimine coordination depended on the wingtip groups at the carbene ligands and was accomplished either by photolytic activation of a carbonyl ligand from the cationic $[Fe(cp)(NHC)(CO)_2]^+$ precursor (alkyl wingtips) or by $AgBF_4$-mediated halide abstraction from the neutral complex [FeI(cp)(NHC)-(CO)] (mesityl wingtips). Remarkably, the polymeric materials were substantially more stable than the related bimetallic model complexes. Electrochemical analyses indicated metal–metal interactions in the pyrazine-containing polymers, whereas in 4,4′-bipyridine-linked systems the metal centers were electronically decoupled.

Introduction

While the impact of *N*-heterocyclic carbene (NHC) complexes in catalysis has been widely recognized,[1] the application of organometallic NHC chemistry in other areas of materials science has been much less developed thus far.[2–4] This is remarkable, especially when considering the relatively robust metal–carbon bond in NHC complexes.[5] In addition, theoretical[6] and experimental[7] results have indicated that the M–C_{NHC} bond comprises a significant portion of π character when bound to electron-rich metal centers. Such bonding may become attractive for designing systems for potential applications in molecular electronics, since facile transfer of electron density along π networks may also encompass the metal center. Specifically when using redox-active metal centers in the main-chain, organometallic polymers have great potential to surpass the versatility of most common organic or inorganic conducting systems,[8] as the oxidation state of the metal center in these organometallic polymers represents an additional function that can be selectively addressed and reversibly switched.

Initial efforts on using organometallic NHC chemistry for polymer synthesis concentrated on metals with low redox activity.[9] Predominantly, through the pioneering work of Bielawski and coworkers, a range of ditopic carbene ligands became available for the interconnection of two metal centers.[10] Subsequent exploitation of this approach provided access to redox-active molecular switches[11] and to molecular squares.[12] Stimulated by these achievements, we aimed at expanding the use of ditopic carbene ligands for the fabrication of co-polymers containing redox-active NHC iron(II) units[13] in the main-chain.

Our retrosynthetic approach towards such co-polymers was based on the interconnection of a bimetallic synthon with a ditopic, bridging ligand (Fig. 1). Since coordination of a second, non-chelating NHC ligand to an Fe–NHC complex proved to be difficult, we focused our attention on co-polymers that feature two

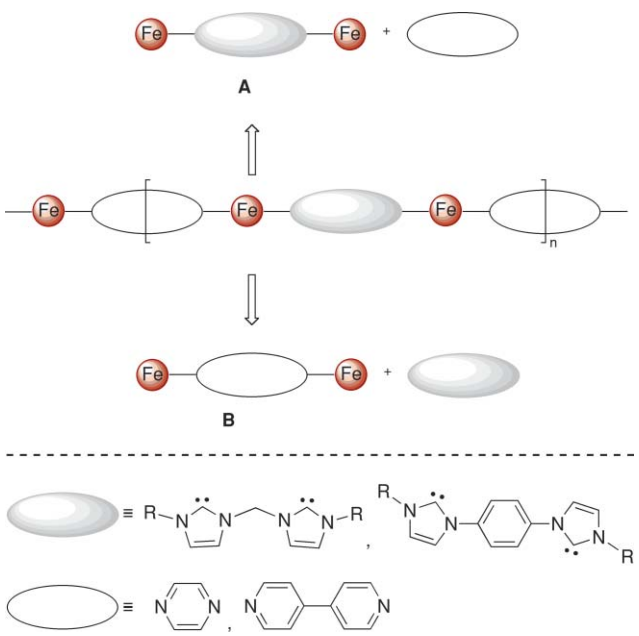

Fig. 1 Retrosynthetic approach towards organometallic polymers comprised of NHC metal complexes in the main-chain.

[a]*Department of Chemistry, University of Fribourg, Chemin du Musee 9, CH-1700 Fribourg, Switzerland. E-mail: martin.albrecht@unifr.ch; Fax: +41 263009738; Tel: +41 263008786*
[b]*XRD Application Lab, CSEM, Rue Jaquet Droz 1, CH-2000 Neuchâtel, Switzerland*
[c]*Institute of Physics, University of Neuchâtel, rue Emile-Argand 11, CH-2009 Neuchâtel, Switzerland*
[d]*School of Chemistry and Chemical Biology, University College Dublin Belfield, Dublin 4, Ireland*

† CCDC reference numbers 726548–726552. For crystallographic data in CIF or other electronic format see DOI: 10.1039/b907018d

different interconnecting ligands. Hence, the desired co-polymer can be dissected into two bimetallic synthons **A** and **B** (Fig. 1), each comprising a different ditopic ligand. Here we report on the synthesis and electrochemical properties of iron NHC polymers and their bimetallic synthons **A** and **B**. Metal–metal interactions in these systems are strongly dependent on the type of diimine ligand employed.

Experimental section

General comments

All manipulations were performed using standard Schlenk techniques under an argon atmosphere unless stated otherwise. Toluene, THF and CH_2Cl_2 were dried by passage through solvent purification columns, all other reagents were used without further purification. The synthesis of the diimidazolium salts **1**[14] and **2**[15] and complexes **7**[13] and **8**[16] are described elsewhere. Unless otherwise stated, all ^1H and $^{13}C\{^1H\}$ NMR spectra were recorded at 25 °C on Bruker spectrometers operating at 360 or 400 MHz (^1H NMR) and at 100 MHz (^{13}C NMR), respectively. Resonance frequencies were referenced to residual solvent ^1H or ^{13}C resonances. Chemical shifts (δ) are given in ppm, coupling constants (J) in Hz. Assignments are based either on distortionless enhancement of polarization transfer (DEPT) experiments or on homo- and heteronuclear shift correlation spectroscopy. Elemental analyses were performed by the Microanalytical Laboratory of Ilse Beetz (Kronach, Germany) and by the Microanalytical Laboratory of the ETH Zürich (Switzerland). A commercially available Hg lamp was used for irradiation. Absorption spectra were measured on an Agilent 8453 UV-Vis spectrophotometer. IR spectra were recorded on a Mattson 5000 FT-IR and a Bruker Tensor 27 FT-IR instrument for solution and solid state measurements, respectively.

Syntheses

Synthesis of 3. To a suspension of the diimidazolium salt **1** (0.32 g, 0.5 mmol) in dry THF (10 mL) was added *n*BuLi (1.6 M in hexanes, 0.63 mL, 1.0 mmol) at −78 °C. After stirring for 30 min at RT, the mixture was frozen and overlaid with a solution of $[FeI(cp)(CO)_2]$ (0.76 g, 2.5 mmol) in dry toluene (30 mL). The reaction mixture was gradually warmed to RT and stirred for 16 h. The formed precipitate was separated by centrifugation, washed once with dry toluene (30 mL) and then extracted with dry CH_2Cl_2 (2 × 20 mL). The combined CH_2Cl_2 fractions were reduced to *ca.* 20 mL and subsequently irradiated for 16 h. All volatiles were removed *in vacuo*, and the residue was purified by gradient column chromatography (SiO_2, CH_2Cl_2–acetone) and by subsequent precipitation from CH_2Cl_2–pentane. The product was obtained as a green powder (0.32 g, 68%) as a mixture of diastereoisomers. X-Ray quality crystals were grown by slow diffusion of pentane into a CH_2Cl_2 solution of **3** at −20 °C. Analytically pure material was obtained by recrystallisation from toluene–pentane. ^1H NMR of major isomer ($CDCl_3$, 400 MHz): δ 8.49 (s, 2H, NCH_2N), 7.34 (d, $^3J_{HH} = 2.1$ Hz, 2H, H_{NHC}), 7.05, 7.03 (2 × s, 4H, H_{Mes}), 6.79 (d, $^3J_{HH} = 2.1$ Hz, 2H, H_{NHC}), 4.56 (s, 10H, H_{cp}), 2.41 (s, 6H, *p*-CH_3), 1.90, 1.88 (2 × s, 12H, *o*-CH_3). ^1H NMR of minor isomer ($CDCl_3$, 400 MHz): δ 8.42, 8.20 (2 × d, $^2J_{HH} = 12.8$ Hz, 2H, NCH_2N), 7.81, 7.08 (2 × d, $^3J_{HH} = 2.1$ Hz, 2H, H_{NHC}), 7.05, 7.03 (2 × s, 4H, H_{Mes}), 7.01, 6.92 (2 × d, $^3J_{HH} = 2.1$ Hz, 2H, H_{NHC}), 4.47 (s, 10H, H_{cp}), 2.42 (s, 6H, *p*-CH_3), 1.97, 1.94, 1.92 (3 × s, 12H, *o*-CH_3). $^{13}C\{^1H\}$ NMR ($CDCl_3$, 100 MHz): δ 220.3 (CO), 192.1 ($C_{carbene}$), 139.7, 138.1, 137.0, 134.7 (4 × C_{Mes}), 129.9, 129.1 (2 × C_{Mes}–H), 124.6, 124.1 (2 × C_{NHC}–H), 80.2 (C_{cp}), 68.8 (NCH_2N), 21.4, 18.6, 18.0 (3 × CH_3). IR (neat, cm^{-1}): 1939 ν(CO). Anal. Calcd for $C_{37}H_{38}Fe_2I_2N_4O_2$ (936.22) × 1/2 $C_6H_5CH_3$: C 49.52, H 4.31, N 5.70. Found: C 49.49, H 4.28, N 5.67.

Synthesis of 4. To a suspension of the diimidazolium salt **2** (1.16 g, 2.0 mmol) in dry THF (20 mL) was added $LiN(SiMe_3)_2$ (1 M in THF, 4.0 mL, 4.0 mmol) at RT. After stirring for 1 h, this solution was added to a solution of $[FeI(cp)(CO)_2]$ (1.15 g, 3.8 mmol) in dry toluene (40 mL) and stirring was continued for 16 h. The formed precipitate was separated by centrifugation, washed once with dry toluene (30 mL) and then with dry CH_2Cl_2 (2 × 20 mL). The product was obtained as a yellow powder (0.31 g, 67%). Single crystals suitable for X-ray diffraction analysis were grown in the dark by slow Et_2O diffusion into a $MeNO_2$ solution. ^1H NMR (DMSO-d_6, 400 MHz): δ 7.99 (s, 2H, H_{NHC}), 7.78 (br, 6H, H_{Ph} and H_{NHC}), 5.45 (s, 10H, H_{cp}), 4.23 (br, 4H, NCH_2), 1.89 (br, 4H, NCH_2CH_2), 1.50 (br, 4H, CH_2CH_3), 1.01 (t, $^3J_{HH} = 7.2$ Hz, 6H, CH_2CH_3). $^{13}C\{^1H\}$ NMR (DMSO-d_6, 100 MHz): δ 211.6 (CO), 165.8 ($C_{carbene}$), 140.8 (C_{Ph}), 130.0 (C_{Ph}–H), 128.3, 125.1 (2 × C_{NHC}–H), 87.8 (C_{cp}), 51.1 (NCH_2), 32.3 (NCH_2CH_2), 19.3 (CH_2CH_3), 13.8 (CH_2CH_3). IR (neat, cm^{-1}): 2049, 1981 ν(CO). Anal. Calcd for $C_{34}H_{36}Fe_2I_2N_4O_4$ (930.17): C 43.90, H 3.90, N 6.02. Found: C 43.79, H 3.98, N 5.98.

Synthesis of 5. Complex **4** (0.28 g, 0.3 mmol) and $AgBF_4$ (0.12 g, 0.6 mmol) were stirred in $MeNO_2$ and CH_2Cl_2 (20 mL, 1 : 1 v/v) in the dark for 3 h. The suspension was filtered through Celite and evaporated to dryness, affording the crude product as a yellow powder (0.24 g, 96%). An analytically pure sample was obtained by recrystallisation of **5** from $MeNO_2$–Et_2O. ^1H NMR (DMSO-d_6, 360 MHz): δ 7.99 (s, 2H, H_{NHC}), 7.78 (s, 6H, H_{Ph} and H_{NHC}), 5.44 (s, 10H, H_{cp}), 4.22 (br, 4H, NCH_2), 1.88 (br, 4H, NCH_2CH_2), 1.50 (br, 4H, CH_2CH_3), 1.01 (t, $^3J_{HH} = 7.3$ Hz, 6H, CH_2CH_3). IR (neat, cm^{-1}): 2051, 1984 ν(CO). Anal. Calcd for $C_{34}H_{36}B_2F_8Fe_2N_4O_4$ (849.97) × 1/4 $MeNO_2$: C 47.54, H 4.28, N 6.88. Found: C 47.57, H 4.63, N 7.14.

Synthesis of 6. A solution of **4** (0.186 g, 0.2 mmol) in dry CH_2Cl_2 (10 mL) was irradiated for 16 h, upon which the initially yellow solution became green. Evaporation of the solvent gave the crude product as a green powder, which was purified by precipitation from CH_2Cl_2–pentane (0.14 g, 80%). Recrystallisation from CH_2Cl_2–toluene–Et_2O at +4 °C gave an analytically pure sample. ^1H NMR ($CDCl_3$, 400 MHz): δ 7.33 (d, $^3J_{HH} = 2.0$ Hz, 2H, $H_{NHC\ minor}$), 7.31 (d, $^3J_{HH} = 2.0$ Hz, 2H, $H_{NHC\ major}$), 7.30–7.13 (br, 4H, H_{Ph}), 7.21 (d, $^3J_{HH} = 2.0$ Hz, 2H, $H_{NHC\ minor}$), 7.09 (d, $^3J_{HH} = 2.0$ Hz, 2H, $H_{NHC\ major}$), 5.10–4.95, 4.91–4.79 (2 × m, 4H, NCH_2), 4.44, 4.43 (2 × s, 10H, H_{cp}), 2.13–1.87 (2 × m, 4H, NCH_2CH_2), 1.73–1.56 (m, 4H, CH_2CH_3), 1.11 (t, $^3J_{HH} = 7.4$ Hz, 6H, CH_2CH_3). $^{13}C\{^1H\}$ NMR ($CDCl_3$, 100 MHz): δ 222.5, 221.7 (2 × CO), 189.1, 188.8 (2 × $C_{carbene}$), 142.3, 142.1 (2 × C_{Ph}), 129.2, 128.4 (2 × C_{Ph}–H), 125.6, 125.4, 123.0, 122.9 (4 × C_{NHC}–H), 80.5, 80.4 (2 × C_{cp}), 54.1, 54.0 (2 × NCH_2), 33.6, 33.6 (2 × NCH_2CH_2), 20.4 (CH_2CH_3),

14.3 (CH_2CH_3). IR (CH_2Cl_2, cm^{-1}): 1941 ν(CO). Anal. Calcd for $C_{32}H_{36}Fe_2I_2N_4O_2$ (874.15) × $C_6H_5CH_3$: C 46.33, H 4.38, N 6.09. Found: C 46.29, H 4.74, N 6.10.

Synthesis of 9a. A solution of **7** (0.208 g, 0.5 mmol) and pyrazine (0.020 g, 0.25 mmol) in dry CH_2Cl_2 (10 mL) was irradiated for 16 h. During this time the initially yellow solution turned purple and a precipitate formed. Separation of the precipitate by filtration and washing with dry CH_2Cl_2 gave **9a** as a purple solid (0.116 g, 54%), which was precipitated from $MeNO_2$–acetone–Et_2O at 0 °C to give an analytically pure sample. ^{1}H NMR ($MeNO_2$-d_3, 400 MHz, 258 K): δ 8.12–7.63 (br, 4H, H_{pz}), 7.63–7.40 (m, 4H, H_{NHC}), 5.1–4.9 (br, 2H, $CHMe_2$), 4.98 (s, 10H, H_{cp}), 4.78–4.60 (br, 2H, $CHMe_2$), 1.71–1.57, 1.57–1.43, 1.43–1.27, 0.85–0.66 (4 × m, 24H, $CH(CH_3)_2$). $^{13}C\{^1H\}$ NMR ($MeNO_2$-d_3, 100 MHz, 258 K): δ 221.8 (CO), 174.3 ($C_{carbene}$), 153.9 (C_{pz}–H), 123.2, 122.7 (2 × C_{NHC}–H), 85.4 (C_{cp}), 54.2, 53.5 (2 × $CHMe_2$), 24.4, 23.9, 23.5, 22.3 (4 × $CH(CH_3)_2$). The resonances of the second isomer are strongly overlapping, additional signals were detected at δ_C 221.7 (CO), 174.4 ($C_{carbene}$), 85.4 (C_{cp}), 54.3, 53.4 (2 × $CHMe_2$). IR (neat, cm^{-1}): 1952 ν(CO). Anal. Calcd for $C_{34}H_{46}B_2F_8Fe_2N_6O_2$ (856.07): C 47.70, H 5.42, N 9.82. Found: C 47.61, H 5.48, N 9.83.

Synthesis of 9b. To a solution of **8** (0.174 g, 0.3 mmol) and pyrazine (0.013 g, 0.17 mmol) in dry CH_2Cl_2 (10 mL) was added $AgBF_4$ (0.058 g, 0.3 mmol) and the resulting suspension was stirred for 16 h. During this time the initially yellow solution turned red and a precipitate formed. Separation of the precipitate by filtration and subsequent repeated precipitation from CH_2Cl_2–$MeNO_2$–Et_2O at 0 °C gave **9b** as an analytically pure solid (0.110 g, 63%). Crystals suitable for an X-ray diffraction analysis were obtained from acetone–pentane at +4 °C. ^{1}H NMR ($MeNO_2$-d_3, 400 MHz, 258 K): δ 7.48 (s, 4H, H_{NHC}), 7.44 (s, 4H, H_{pz}), 7.26, 6.85 (2 × s, 8H, H_{Mes}), 4.72 (s, 10H, H_{cp}), 2.43, 2.28, 1.53 (3 × s, 36H, CH_3). $^{13}C\{^1H\}$ NMR ($MeNO_2$-d_3, 100 MHz, 258 K): δ 219.3 (CO), 177.2 ($C_{carbene}$), 153.3 (C_{pz}–H), 141.9, 137.7, 137.2 (3 × C_{Mes}), 131.0, 129.9 (2 × C_{Mes}–H), 129.5 (C_{NHC}–H), 85.5 (C_{cp}), 21.2, 18.7, 17.9 (3 × CH_3). IR (neat, cm^{-1}): 1946 ν(CO). Anal. Calcd for $C_{58}H_{62}B_2F_8Fe_2N_6O_2$ (1160.45) × 1/2 CH_2Cl_2: C 58.41, H 5.28, N 6.99. Found: C 58.85, H 5.33, N 7.10.

Synthesis of 10a. This complex was prepared in a manner similar to that for **9a** using **7** (0.38 g, 0.9 mmol) and 4,4′-bipyridine (0.071 g, 0.46 mmol) in degassed acetone (20 mL). Precipitation gave an analytically pure red solid (0.174 g, 41%). ^{1}H NMR ($MeNO_2$-d_3, 400 MHz, 258 K): δ 8.22 (br, 4H, H_{bpy}), 7.60–7.4 (br, 4H, H_{NHC}), 7.42 (d, $^3J_{HH}$ = 6.9 Hz, 4H, H_{bpy}), 5.22 (br, 2H, $CHMe_2$), 4.99 (s, 10H, H_{cp}), 4.93 (br, 2H, $CHMe_2$), 1.63, 1.50, 1.39, 0.49 (4 × s, 24H, $CH(CH_3)_2$). $^{13}C\{^1H\}$ NMR ($MeNO_2$-d_3, 100 MHz, 258 K): δ 223.6 (CO), 177.0 ($C_{carbene}$), 159.8 (C_{bpy}–H), 145.1 (C_{bpy}), 123.7 (C_{bpy}–H), 122.8, 122.3 (2 × C_{NHC}–H), 84.3 (C_{cp}), 54.0, 53.4 (2 × $CHMe_2$), 24.4, 23.9, 23.6, 21.8 (4 × $CH(CH_3)_2$). IR (neat, cm^{-1}): 1937 ν(CO). Anal. Calcd for $C_{40}H_{50}B_2F_8Fe_2N_6O_2$ (932.16) × 1/2 CH_2Cl_2: C 49.91, H 5.27, N 8.62. Found: C 49.72, H 5.47, N 8.87.

Synthesis of 10b. This complex was prepared in a manner similar to that for **9b** using **8** (0.174 g, 0.3 mmol), 4,4′-bipyridyl (0.027 g, 0.17 mmol) and $AgBF_4$ (0.058 g, 0.3 mmol) in dry CH_2Cl_2 (10 mL). The reaction mixture was filtered through Celite at 0 °C, evaporated to dryness and then precipitated twice from CH_2Cl_2–$MeNO_2$–Et_2O at 0 °C to give an analytically pure orange solid (0.104 g, 56%). ^{1}H NMR ($MeNO_2$-d_3, 400 MHz, 258 K): δ 8.18 (s, 4H, H_{bpy}), 7.48 (s, 4H, H_{NHC}), 7.30 (s, 4H, H_{Mes}), 7.18 (s, 4H, H_{bpy}), 6.95–6.71 (m, 4H, H_{Mes}), 4.61 (s, 10H, H_{cp}), 2.80–1.79, 1.64–1.27 (2 × m, 36H, CH_3). $^{13}C\{^1H\}$ NMR ($MeNO_2$-d_3, 100 MHz, 258 K): δ 220.7 (CO), 180.8 ($C_{carbene}$), 160.5 (C_{bpy}–H), 144.6 (C_{bpy}), 141.4, 137.6 (2 × C_{Mes}), 130.7, 130.3 (2 × C_{Mes}–H), 129.0 (C_{NHC}–H), 122.8 (C_{bpy}–H), 84.3 (C_{cp}), 21.2, 18.7, 17.8 (3 × CH_3). IR (neat, cm^{-1}): 1947 ν(CO). Anal. Calcd for $C_{64}H_{66}B_2F_8Fe_2N_6O_2$ (1236.55) × 3/4 CH_2Cl_2: C 59.81, H 5.23, N 6.46. Found: C 59.79, H 5.28, N 6.69.

Synthesis of 11. Irradiation of a solution of **7** (0.17 g, 0.4 mmol) in dry MeCN (10 mL) for 16 h and subsequent solvent evaporation gave **11** as an orange solid in quantitative yield (0.18 g). Analytically pure material was obtained by recrystallisation of **11** from CH_2Cl_2–Et_2O at +4 °C. ^{1}H NMR (acetone-d_6, 400 MHz): δ 7.74 (s, 2H, H_{NHC}), 5.35–5.05 (br, 2H, $CHMe_2$), 4.96 (s, 5H, H_{cp}), 2.46 (s, 3H, CH_3CN), 1.59, 1.41 (2 × d, $^3J_{HH}$ = 6.7 Hz, 12H, $CH(CH_3)_2$). $^{13}C\{^1H\}$ NMR (acetone-d_6, 100 MHz): δ 221.4 (CO), 173.7 ($C_{carbene}$), 136.1 (CH_3CN), 122.4 (C_{NHC}–H), 83.2 (C_{cp}), 53.1 ($CHMe_2$), 23.8, 23.7 (2 × $CH(CH_3)_2$), 4.8 (CH_3CN). IR (neat, cm^{-1}): 1964 ν(CO). Anal. Calcd for $C_{17}H_{24}BF_4FeN_3O$ (429.04): C 47.59, H 5.64, N 9.79. Found: C 47.72, H 5.46, N 9.68.

Synthesis of 12. In analogy to the preparation of **5**, irradiation of a solution of **7** (0.11 g, 0.3 mmol) and pyridine (0.11 g, 1.3 mmol) in dry CH_2Cl_2 (10 mL) for 16 h and subsequent evaporation of the volatiles yielded the crude product as a dark brown solid in quantitative yield (0.13 g). Recrystallisation from acetone–pentane at +4 °C gave an analytically pure sample. ^{1}H NMR (acetone-d_6, 400 MHz): δ 8.26 (d, $^3J_{HH}$ = 5.3 Hz, 2H, o-H_{py}), 7.81 (m, 1H, p-H_{py}), 7.74 (s, 2H, H_{NHC}), 7.27 (m, 2H, m-H_{py}), 5.20 (m, 2H, $CHMe_2$), 5.10 (s, 5H, H_{cp}), 1.63 (d, $^3J_{HH}$ = 6.5 Hz, 6H, $CH(CH_3)_2$), 0.99 (br, 6H, $CH(CH_3)_2$). $^{13}C\{^1H\}$ NMR (acetone-d_6, 100 MHz): δ 223.4 (CO), 177.3 ($C_{carbene}$), 159.1 (o-C_{py}–H), 138.6 (p-C_{py}–H), 126.8 (m-C_{py}–H), 122.7 (C_{NHC}–H), 83.8 (C_{cp}), 53.3 ($CHMe_2$), 24.2, 22.7 (2 × $CH(CH_3)_2$). IR (neat, cm^{-1}): 1927 ν(CO). Anal. Calcd for $C_{20}H_{26}BF_4FeN_3O$ (467.09): C 51.43, H 5.61, N 9.00. Found: C 51.65, H 5.55, N 9.12.

General procedure for the preparation of polymers 13a and 14a. An acetone solution (10 mL) containing complex **5** (0.15 mmol) and diimine (0.15 mmol) was irradiated for 16 h. The product precipitated from the reaction mixture and was collected by filtration and washed with CH_2Cl_2 (2 × 2 mL). Analytical data are collected in Table 1.

Table 1 Spectroscopic and electrochemical data for polymers **13** and **14**

				Elem. anal.		
	ν_{CO} [a]	λ_{max} [b]	$E_{1/2}$ (ΔE_p) [c]	C	H	N
13a	1969	420 (sh), 568	1.23 (broad)	46.76	4.53	7.69
13b	1961	419, 537	1.26 (broad)	49.94	4.80	8.26
14a	1937 [d]	470	0.97 (177)	51.93	4.53	8.59
14b	1960	444	1.09 (163)	52.86	4.73	7.98

[a] In cm^{-1}, measured neat.
[b] In nm, measured in $MeNO_2$.
[c] In V, measured in $MeNO_2$ and calibrated to Fc^+/Fc ($E_{1/2}$ = 0.35 V *vs.* SCE) as internal standard, $\Delta E_p = E_{pa} - E_{pc}$ in mV.
[d] Additional shoulders at 1975 and 1963 cm^{-1}.

Table 2 Crystallographic data for complexes **3**, **4**, **9b**, **11**, and **12**

	3	**4**	**9b**	**11**	**12**
Color, shape	Green block	Yellow rod	Red rod	Red prism	Red block
Size/mm	$0.50 \times 0.40 \times 0.35$	$0.45 \times 0.25 \times 0.15$	$0.20 \times 0.13 \times 0.11$	$0.18 \times 0.15 \times 0.13$	$0.23 \times 0.18 \times 0.16$
Empirical formula	$C_{37}H_{38}Fe_2I_2N_4 \times CH_2Cl_2$	$C_{34}H_{36}Fe_2I_2N_4O_4$	$C_{58}H_{62}B_2F_8Fe_2N_6O_2 \times 2\ C_3H_6O$	$C_{17}H_{24}BF_4FeN_3O$	$C_{20}H_{26}BF_4FeN_3O$
Fw	1021.14	930.17	1276.61	429.05	467.10
T/K	173(2)	173(2)	173(2)	160(1)	173(2)
Crystal system	Triclinic	Triclinic	Monoclinic	Monoclinic	Monoclinic
Space group unit cell	$P\bar{1}$ (No. 2)	$P\bar{1}$ (No. 2)	$P2_1/c$ (No. 14)	$P2_1/n$ (No. 14)	$P2_1/n$ (No. 14)
a/Å	11.6665(8)	7.8161(13)	12.1129(17)	9.3055(2)	11.7156(9)
b/Å	12.7160(7)	9.7331(15)	20.0683(19)	21.7066(4)	14.0710(7)
c/Å	15.2275(8)	12.836(2)	14.218(2)	10.3747(2)	13.7433(10)
α/°	66.698(4)	99.738(13)	90.00	90.00	90.00
β/°	87.838(5)	104.479(13)	115.165(11)	108.404(1)	105.542(6)
γ/°	79.813(5)	89.843(13)	90.00	90.00	90.00
V/Å^3	2040.8(2)	931.1(3)	3128.1(7)	1988.41(7)	2182.7(3)
Z	2	1	2	4	4
D_{calc}/g cm^{-3}	1.662	1.659	1.355	1.433	1.421
μ/mm^{-1} (Mo Kα)	2.391	2.477	0.539	0.806	0.740
Measured reflections	26 602	8252	14 935	45 202	30 379
Unique reflections, R_{int}	10 857, 0.092	3307, 0.085	4089, 0.135	4541, 0.101	5895, 0.060
Observed reflections, [$I > 2\sigma(I)$]	9449	2608	2168	3725	3905
Transmission range	0.054–0.483	0.366–0.912	0.992–1.010	0.757–0.906	0.984–1.016
no. parameters, restraints	430, 0	209, 0	396, 0	249, 0	330, 0
R,[a] wR,[b]	0.082, 0.231	0.060, 0.155	0.053, 0.074	0.054, 0.129	0.032, 0.060
GOF	1.024	0.982	0.824	1.141	0.831
Min., max. residual densities/e Å^{-3}	–3.559, 2.160	–1.504, 1.199	–0.235, 0.259	–0.509, 0.575	–0.309, 0.284

[a] $R_1 = \sum\|F_o| - |F_c\|/\sum|F_o|$ for all $I > 2\sigma(I)$. [b] $wR_2 = [\sum w(F_o^2 - F_c^2)^2/\sum(w(F_o^4)]^{1/2}$.

General procedure for the preparation of polymers 13b and 14b. Complex **3** (0.15 mmol), diimine (0.15 mmol) and $AgBF_4$ (0.33 mmol) were stirred in dry CH_2Cl_2 (10 mL) for 16 h. The reaction mixture was filtered through Celite, evaporated to dryness and then precipitated twice from CH_2Cl_2–$MeNO_2$–Et_2O to give the desired polymers. Analytical data are collected in Table 1.

Electrochemical measurements

Electrochemical studies were carried out using an EG & G Princeton Applied Research Potentiostat Model 273A employing a gastight three-electrode cell under an argon atmosphere. For compounds **3**, **6**, **11** and **12** a Pt disk with a 3.80 mm^2 surface area or a glassy-carbon disk with a 3.14 mm^2 surface area was used as the working electrode and was polished before each measurement. The reference was a Ag/AgCl electrode; the counter electrode was a Pt wire. Bu_4NPF_6 (0.1 M) in dry CH_2Cl_2 was used as a base electrolyte with analyte concentrations of approximately 1×10^{-3} M. Measurements were carried out at RT and at 100 mV s^{-1} sweep rates unless stated otherwise. The redox potentials were measured against ferrocenium/ferrocene (Fc^+/Fc; $E_{1/2} = 0.46$ V *vs.* SCE)[17] or against $[Ru(bpy)_3]^{3+}/[Ru(bpy)_3]^{2+}$ ($E_{1/2} = 1.39$ V *vs.* SCE),[18] which were used as internal standards. For compounds **9**, **10**, **13** and **14** a similar setup was used except that measurements were carried out in $MeNO_2$ at –20 °C and referenced to Fc^+/Fc as the internal standard ($E_{1/2} = 0.35$ V *vs.* SCE in $MeNO_2$).

Crystal structure determination†

Suitable single crystals were mounted on a Stoe Mark II-Imaging Plate Diffractometer System (Stoe & Cie, 2002; for **3**, **4**, **9b** and **12**) and on a Nonius KappaCCD area-detector diffractometer (for **11**) equipped with a graphite-monochromator. Data collections were performed at –100 °C (for **3**, **4**, **9b** and **12**) and at –113 °C (for **11**) using Mo Kα radiation ($\lambda = 0.71073$ Å). All structures were solved by direct methods using SHELXS-97[19] (for **3**, **4**, **9b** and **12**) or *SIR92*[20] (for **11**) and refined by full-matrix least-squares on F^2 with SHELXL-97.[19] Hydrogen atoms were included in calculated positions and treated as riding atoms using SHELXL-97 default parameters. All non-hydrogen atoms were refined anisotropically. A semi-empirical absorption correction was applied for **4**, **9b**, **11** and **12** using Sortav[21] or MULscanABS as implemented in PLATON.[22] An empirical absorption correction was applied for **3** using DELrefABS as implemented in PLATON.

For complex **3**, a region of electron density related to a disordered molecule of CH_2Cl_2 was squeezed out using the SQUEEZE routine in PLATON03 (82 electrons for 305.7 Å^3 per unit cell). In complex **12**, the BF_4^- anion is disordered. Further details on data collection and refinement parameters are collected in Table 2. Crystallographic data (excluding structure factors) for the structures **3**, **4**, **9b**, **11**, and **12** have been deposited with the Cambridge Crystallographic Data Centre as ESI CCDC numbers 726548–726552.† Copies of the data can be obtained free of charge on application to CCDS, 12 Union Road, Cambridge CB2 1EZ, UK [Fax: (int.) +44–1223-336–033; E-mail: deposit@ccds.cam.ac.uk].

Results and discussion

Carbene-connected dinuclear iron(II) complexes (synthon A)

Formation of synthon **A** required a ditopic carbene ligand precursor. For this purpose, we investigated the diimidazolium

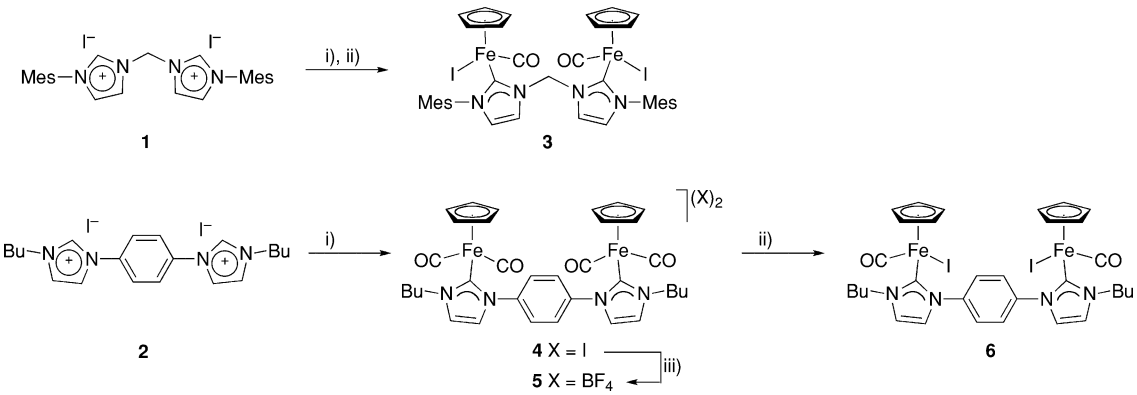

Scheme 1 Synthesis of NHC-interconnected dinuclear iron(II) complexes; reagents and conditions: (i) *n*BuLi or $LiN(SiMe_3)_2$, THF; then $[FeI(cp)(CO)_2]$, toluene; (ii) *hν*, CH_2Cl_2; (iii) $AgBF_4$, $MeNO_2$–CH_2Cl_2.

salts **1** and **2** comprised of a flexible methylene and a rigid phenylene linker, respectively. The bimetallic iron(II) complexes **3–6** containing these bridging NHC ligands were synthesized *via* the free carbene route (Scheme 1). In order to prevent chelation of the flexible dicarbene ligand derived from **1**,[13] metal coordination was performed at low ligand concentrations. After deprotonation of **1** by BuLi in THF, the reaction mixture was thus frozen and overlaid with an excess of the metal precursor $[FeI(cp)(CO)_2]$ dissolved in toluene. Upon gradual melting and warming of the resulting suspension to RT, the bimetallic tetracarbonyl complex formed as a precipitate. Subsequent solvent exchange and irradiation of this intermediate in CH_2Cl_2 yielded the bimetallic neutral complex **3**. Compounds **4–6** featuring a rigid phenylene spacer between the carbene units were synthesized similarly, though freezing of the free carbene solution was redundant, as the ligand cannot adopt a chelating coordination mode. The tetracarbonyl complex **4** was isolated and fully characterized. $AgBF_4$-mediated exchange of the non-coordinating anion from I^- to BF_4^- afforded complex **5**, and photochemically induced CO dissociation from **4** gave the neutral diiron complex **6**.

The bridging coordination mode of the dicarbene ligands in complexes **3–6** was confirmed by the pertinent 1 : 1 cp : imidazole molecular ratio in the ^1H NMR spectra. The ^1H NMR spectrum of complex **3** revealed two partially overlapping sets of signals in approximate 4 : 1 ratio. The presence of diastereomers was rationalized by the fact that the iron centers in **3** are stereogenic and should therefore result in mixtures of *rac* and *meso* forms. Most diagnostic are the resonances due to the methylene protons, which appeared as a singlet (δ_H 8.49) in the major isomer and as an AB doublet at δ_H 8.42 and 8.20 ($^2J_{HH}$ = 12.8 Hz) for the minor component. Based on these splittings, the major isomer was assigned as the *rac* form comprising two iron centers with identical chirality. Since the *ortho* CH_3 groups (δ_H 1.90 and 1.88) and the aryl *meta* protons (δ_H 7.05 and 7.03) of the mesityl wingtip were both mutually diastereotopic on the NMR time scale, fast racemisation at iron seems unlikely. Accordingly, the iron–carbene bonds in these bimetallic complexes are rigid and the metal centers are configurationally stable. The preferred formation of one diastereomer was also noted in related bimetallic rhodium[23] complexes containing bridging dicarbene ligands.

Similar diastereotopic mixtures were observed for complex **6**. In the ^1H NMR spectrum, two overlapping singlets for the cp protons (*ca.* 3 : 1 ratio) were distinguishable and the N-bound methylene protons of the butyl wingtip groups appeared as two higher ordered multiplets. Likewise, two sets of resonances were observed in the ^{13}C NMR spectrum. Since stereogenic centers are lacking in the tetracarbonyl complexes **4** and **5**, only one set of resonances was observed in their ^1H and ^{13}C NMR spectra.

Table 3 Selected bond lengths (Å) of complexes **3** and **4**[a]

	3 (X = I1)	**4** (X = C17)		**3** (X = I1)	**4** (X = C17)
Fe1–C7	1.955(5)	1.983(7)	C7–N1	1.374(7)	1.357(8)
Fe2–C26	1.977(6)	—	C7–N2	1.373(7)	1.364(8)
Fe1–$C_{centroid}$	1.723(4)	1.726(3)	C26–N3	1.352(7)	—
Fe2–$C_{centroid}$	1.724(6)	—	C26–N4	1.357(7)	—
Fe1–C6	1.753(7)	1.792(7)	N1–C8	1.394(7)	1.386(10)
Fe2–C25	1.756(7)	—	N2–C9	1.398(8)	1.373(9)
Fe1–X	2.6155(9)	1.765(8)	N3–C27	1.403(7)	—
Fe2–I2	2.6293(12)	—	N4–C28	1.375(7)	—
			C8–C9	1.319(10)	1.351(10)
			C27–C28	1.340(8)	—

[a] Estimated standard deviations in parentheses.

The bridging coordination mode of the dicarbene ligand was unequivocally confirmed by crystal structure determinations of **3** and **4**. Crystals of **3** contained exclusively the *rac* isomer (Fig. 2), thus corroborating the results deduced from solution measurements. The Fe–$C_{carbene}$ distances are 1.955(5) and 1.977(6) Å, respectively (Table 3), and hence similar to those in related Fe–NHC complexes.[11,13,16,24] The metal–metal separation is 6.812(1) Å. In addition, short intermolecular contacts were found between a

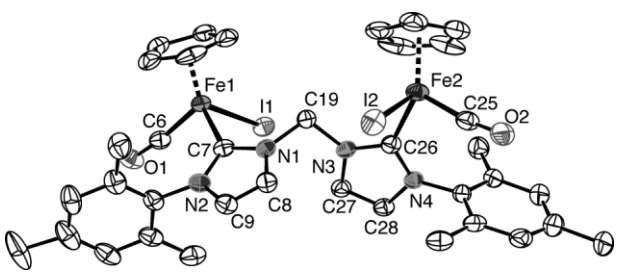

Fig. 2 ORTEP representation and labelling scheme of complex **3** (30% probability ellipsoids; H atoms omitted for clarity).

cp-bound hydrogen and the iodide, which leads to a dimeric structure in the solid state.

In the molecular structure of **4**, the two iron–carbene units are symmetry-related in the solid state (Fig. 3). The Fe–$C_{carbene}$ bond length is 1.983(6) Å and similar to those observed in complex **3**. The metal centers are separated by 8.657(2) Å. Notably, the phenylene ring is arranged nearly orthogonal to the carbene heterocycles, which may be relevant for intramolecular electronic interactions. The large torsion angle (average 78.7(16)°) suggests no overlap between the two π-systems in the ground state.

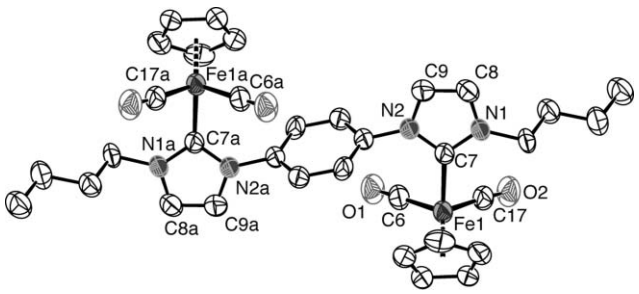

Fig. 3 ORTEP representation of complex **4** (50% probability ellipsoids; H atoms and non-coordinating I^- anions omitted for clarity); a denotes symmetry operation $-x, -y + 3, -z + 2$.

Electrochemical analysis allowed for probing the electronic coupling of the two metal centers in these bimetallic complexes. Cyclic voltammetry (CV) measurements showed a single reversible oxidation for complexes **3** and **6** ($E_{1/2}$ = 0.58 V and 0.47 V *vs.* SCE, respectively; Table 4). These values compare well with other mono- and bimetallic Fe–NHC complexes[13,16] and indicate little or no metal–metal communication. Deconvolution of the differential pulse voltammogram of **6** using the oxidation curve of the related monometallic monocarbene complex suggests two sequential oxidations that are separated by $\Delta E_{1/2}$ = 80 mV. This separation corresponds to a comproportionation constant $K_c = 10^{1.35}$, and hence to a valence-localized, electronically coupled class II system according to the Robin and Day classification.[25] Earlier studies on the monometallic $[Fe(cp)(NHC)(CO)_2]^+$ cation indicated very high oxidation potentials (1.84 V *vs.* SCE) for dicarbonyl derivatives,[13] hence the electrochemical properties of tetracarbonyl complexes **4** and **5** were not analyzed.

Table 4 Spectroscopic and electrochemical data for complexes **3**, **5** and **6**

	ν_{CO}[a]	λ_{max} (ε)[b]	$E_{1/2}$ (ΔE_p)[c]
3	1939	433 (1050), 626 (280)	0.58 (143)
5	2051, 1984	376 (1240)	n.d.[d]
6	1941	n.d.[d]	0.47 (201)

[a] In cm^{-1}, measured neat (**3**, **5**) or in CH_2Cl_2 (**6**).
[b] In nm, measured in CH_2Cl_2 (**3**) or $MeNO_2$ (**5**), ε in cm^{-1} M^{-1}.
[c] In V, measured in CH_2Cl_2, calibrated to $[Ru(bpy)_3]^{3+}/[Ru(bpy)_3]^{2+}$ ($E_{1/2}$ = 1.39 V *vs.* SCE) as internal standard, $\Delta E_p = E_{pa} - E_{pc}$ (in mV).
[d] n.d. = not determined.

Dinuclear Fe(II)–NHC complexes bridged by N-donor ligands (synthon B)

The bimetallic synthon **B** (*cf.* Fig. 1) comprises terminal carbene ligands and a metal–metal bridging diimine system. Accordingly, the bimetallic Fe–NHC complexes **9** and **10** containing an interlinking pyrazine and 4,4′-bipyridine ligand, respectively, were prepared following two different methodologies (Scheme 2). When starting from iron(II) complexes with *i*Pr wingtip groups at the NHC, the dimetallic complexes were most conveniently obtained by photolytic dissociation of one carbonyl ligand from the dicarbonyl complex **7**. Upon irradiation of a CH_2Cl_2 solution of **7** in the presence of the diimine, compounds **9a** and **10a** precipitated as purple and analytically pure solids. When introducing mesityl wingtip groups, similar photochemical initiation failed. Instead, formation of **9b** and **10b** was successfully accomplished from the neutral monocarbonyl complex **8** using $AgBF_4$-mediated halide abstraction followed by coordination of the bridging ligand.

Characteristically, complexes **9** and **10** rapidly change color from purple in the solid state to yellow upon dissolution at RT. This color change is independent of the presence of O_2 or moisture and occurred in coordinating (DMSO, MeCN) as well as in non-coordinating solvents like $MeNO_2$. However, the color change was markedly slower at low temperatures and at high concentrations. UV-Vis spectroscopic analysis of a freshly

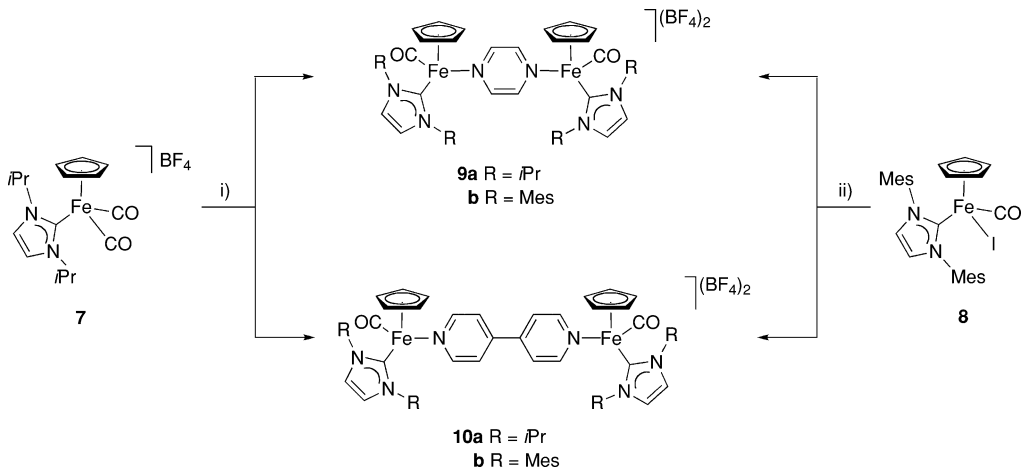

Scheme 2 Synthesis of N-donor-bridged bidentate Fe(II)–NHC complexes; reagents and conditions: (i) pyrazine or 4,4′-bipyridine, *hν*, CH_2Cl_2; (ii) pyrazine or 4,4′-bipyridine, $AgBF_4$, CH_2Cl_2.

prepared $MeNO_2$ solution of **9** featured two absorption maxima located at 434 nm and 578 nm (for **9a**) and 424 nm and 563 nm (for **9b**; Fig. 4(a) and Table 5). Complexes **10a** and **10b** displayed a single maximum at 463 nm and 452 nm, respectively. The absorptions were attributed to charge transfer bands and provided a useful probe for the stability of the complexes. Time-dependent monitoring of the absorption at room temperature indicated that the pyrazine-bridged complex **9a** is considerably less stable than the corresponding bipyridine analogue **10a**. The low energy band of solutions of **9a** completely disappeared in less than 5 min (Fig. 4(b)), while the decrease was much less pronounced for **10a** (Fig. 4(c)).

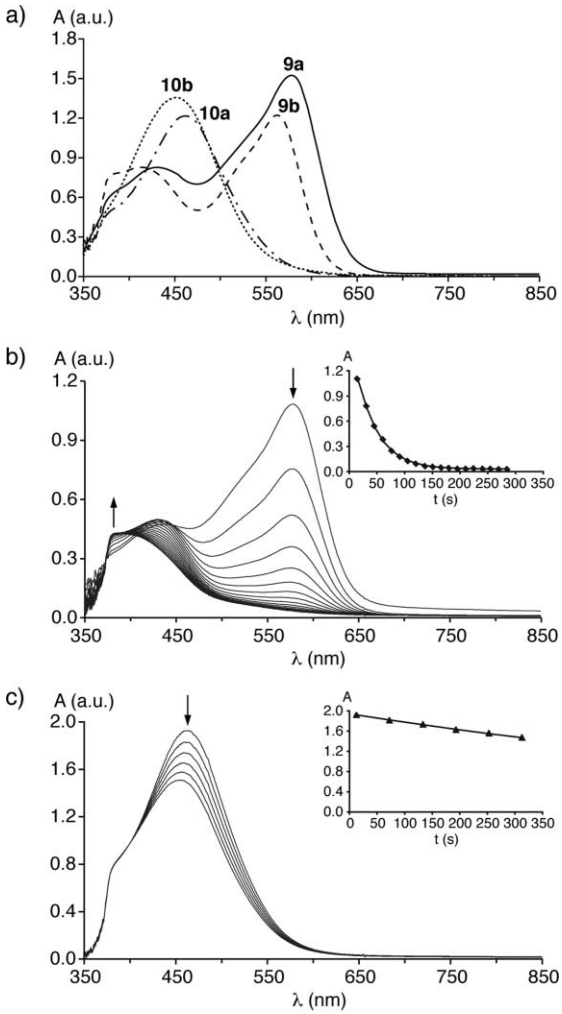

Fig. 4 (a) UV-Vis absorption spectra of bimetallic Fe(II)–NHC complexes **9** and **10** in $MeNO_2$; (b) spectral change of **9a** in $MeNO_2$ at 15 s time increments; inset shows the time-dependent absorption at 578 nm; (c) spectral change of **10a** in $MeNO_2$ at 60 s time increments; inset shows the time-dependent absorption at 463 nm.

Concomitant ^{1}H NMR spectroscopy indicated the gradual formation of free pyrazine from solutions of complex **9a** in $MeNO_2$-d_3. Pyrazine dissociation was evidenced by the decrease of the signal at δ_H 7.82, assigned to bridging pyrazine coordination. The transient appearance of two signals (δ_H 8.23 and 8.26) suggested the formation of an intermediate complex comprising probably of an end-on bound rather than a bridging pyrazine

Table 5 Spectroscopic and electrochemical data of complexes **9** and **10**

	ν_{CO}[a]	λ_{max} (ε)[b]	$E_{1/2}$ (ΔE_p)[c]	$\Delta E_{1/2}$[d]	logK_c[e]
9a	1952	434, 578	1.06 (107), 1.28 (122)	216	3.66
9b	1946	424, 563	1.18 (97), 1.53 (117)	352	5.97
10a	1937	463	0.94 (136)	—	—
10b	1947	452	0.98 (111)	—	—

[a] In cm^{-1}, measured neat.
[b] In nm, measured in $MeNO_2$ (ε not determined due to gradual complex decomposition, see text).
[c] In V, measured in $MeNO_2$ and calibrated to Fc^+/Fc ($E_{1/2}$ = 0.35 V *vs.* SCE) as internal standard, $\Delta E_p = E_{pa} - E_{pc}$ (in mV).
[d] In mV.
[e] Calculated according to log$K_c = \Delta E_{1/2}/59$ mV.

iron complex. Eventual complex decomposition was noted by the growth of the signal at δ_H 8.56, diagnostic for unbound pyrazine, and by the formation of an imidazolium salt. This result correlates well with the observed color change and suggests rapid complex decomposition already at room temperature. Consequently, further analyses of complexes **9** and **10** in solution were carried out at low temperature. In the ^{1}H NMR spectrum of **9a**, recorded at −15 °C in $MeNO_2$-d_3, the pyrazine bridge appeared as a broad signal, which sharpened upon increasing the temperature to RT and which was associated to fluxional behavior of the bridging ligand. Notably, no line broadening was observed for **9b** presumably because the mesityl substituents lock the conformation of the pyrazine. Similarly, the resonances due to the bipyridine ligand in complexes **10** were well resolved. At low temperature, rotation about the N–$C_{wingtip}$ bond appeared to be hindered[13] and each CH_3 group of the *i*Pr and mesityl substituents gave rise to a distinct resonance. The $C_{carbene}$ chemical shifts of **9** and **10** appeared between δ_C 174.3 and 180.8, a typical range for iron(II)-bound NHC carbons.[13,16] While no diastereoisomers due to the chirality at iron were detected by ^{1}H NMR spectroscopy, the ^{13}C NMR spectrum of complex **9a** revealed a second set of signals. The chemical shift differences were generally small (< 0.2 ppm) and some signals were overlapping. The largest differences were observed for the chemical shifts of C_{cp}, C_{CO} and $C_{carbene}$, *i.e.* the nuclei directly attached to and hence most affected by the stereogenic center.

The structure of the pyrazine-bridged dimetallic complex **9b** was analyzed by single crystal X-ray diffraction. Suitable crystals were grown at 4 °C from $MeNO_2$–Et_2O solution. Perhaps the most remarkable feature of the molecular structure of **9b** consists of the π interactions between the pyrazine heterocycle and two mesityl wingtip groups, one from each NHC ligand (Fig. 5). The interplanar separation is 3.664(3) Å, which is at the upper limit for π–π interactions (typical distances are 3.4–3.6 Å).[26] The metal–metal separation in this rigid system is 6.8218(17) Å.

The CV of **9a** in $MeNO_2$ at −20 °C revealed two reversible waves centered at $E_{1/2}$ = 1.06 V and 1.28 V, indicating electronic coupling between the metal centers (Fig. 6).‡ The separation of the two oxidation processes is 216 mV, which corresponds to a comproportionation constant $K_c = 10^{3.66}$ (class II/III system;

‡ From CV measurements, a 1 : 1 electron oxidation process is not evident for **9a**. However, the DPV signals, albeit weak, show nearly identical peak currents for the oxidations at 1.06 and 1.28 V, consistent with two sequential one-electron processes.

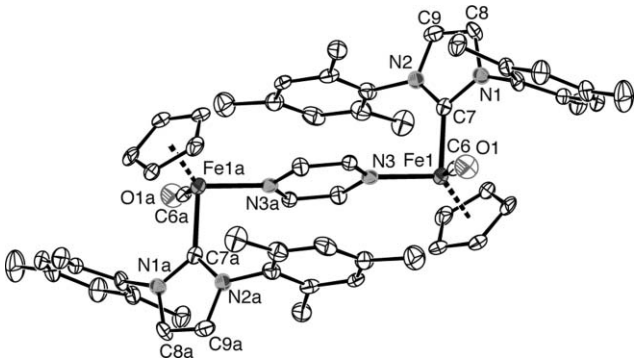

Fig. 5 ORTEP representation of **9b** (50% probability ellipsoids; H atoms, solvent molecules and BF_4^- anions omitted for clarity); a denotes symmetry operation $-x + 2, -y, -z + 1$. Selected bond lengths (Å): Fe1LFe1a 6.8218(17), Fe1–C7 1.977(5), Fe1–$C_{centroid}$ 1.735(3), Fe1–C6 1.741(6), Fe1–N3 1.994(4), C7–N1 1.381(6), C7–N2 1.363(6), N1–C8 1.386(6), N2–C9 1.390(6), C8–C9 1.324(7); selected bond angles (°): C7–Fe1–N3 95.4(2), C7–Fe1–C6 95.6(2), C6–Fe1–N3 94.9(2), N1–C7–N2 102.3(4).

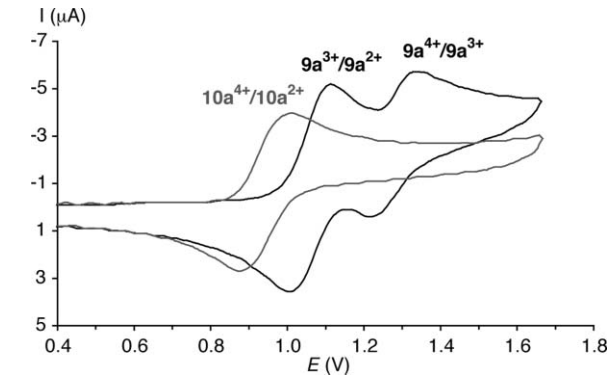

Fig. 6 Cyclic voltammetry diagram of complexes **9a** and **10a** in $MeNO_2$ at –20 °C (100 mV s^{-1} scan rate, Bu_4NPF_6 as supporting electrolyte, glassy carbon working electrode).

Table 5). Complex **9b** undergoes two consecutive and *quasi*-reversible oxidations at $E_{1/2} = 1.18$ V and 1.53 V. The larger separation between the redox processes ($\Delta E = 352$ mV) translates to $K_c = 10^{5.97}$, thus identifying complex **9b** as a class III compound in which the metal centers are coupled and valence delocalized. In contrast, the CV of complexes comprising bridging bipyridine showed a single reversible oxidation only ($E_{1/2} = 0.94$ V for **10a** and $E_{1/2} = 0.98$ V for **10b**), suggesting electronically decoupled metal centers. The electron delocalization observed for the pyrazine-bridged complexes **9** may be a consequence of the favorable overlap between the metal d_π orbitals and the π-system of the pyrazine ligand. Such overlap seems to be more pronounced in **9b** than in **9a**, probably due to the locked conformation of the pyrazine ligand (*cf.* NMR X-ray analyses). Such overlap is absent in the bipyridine complexes **10**.

In order to investigate the binding properties of imine donors to the $[Fe(CO)cp(carbene)]^+$ fragment, the mononuclear Fe–NHC complexes **11** and **12** containing a MeCN and a pyridine ligand, respectively, were synthesized. These complexes were obtained by irradiation of the dicarbonyl precursor **7** in dry MeCN as solvent, or in dry CH_2Cl_2 in the presence of excess pyridine (Scheme 3).§

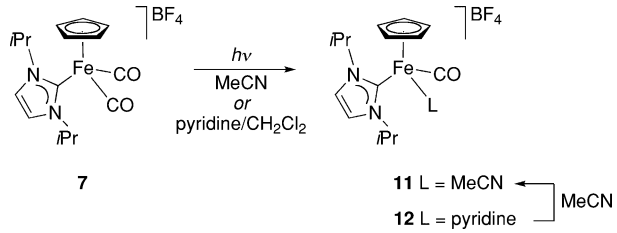

Scheme 3 Synthesis of monodentate Fe(II)–NHC model complexes.

An X-ray diffraction analysis of complexes **11** and **12** did not uncover any unexceptional features (Fig. 7, Table 6). It is worth noting, however, that crystals of **11** were obtained by recrystallization of the diimine complex **9a** from MeCN–Et_2O.

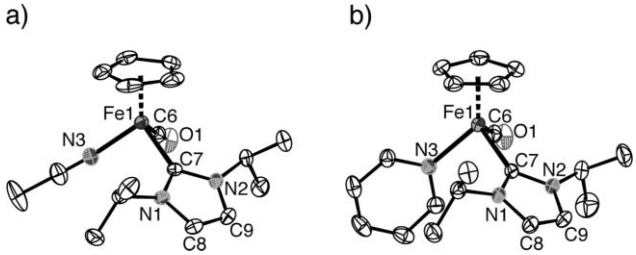

Fig. 7 ORTEP representation of **11** (a; 50% probability ellipsoids, H atoms and BF_4^- anion omitted for clarity) and **12** (b; 50% probability ellipsoids, H atoms and BF_4^- anion omitted for clarity).

Further investigation on the stability of the pyridine ligand in **12** supported the lability of the imine donor. Thus, addition of small amounts of MeCN to an acetone-d_6 solution of the pyridine complex **12** induced the instantaneous appearance of signals identical to those of **11** along with those of free pyridine. These results suggest that MeCN binds significantly stronger to the $[Fe(CO)(cp)(carbene)]^+$ fragment than pyridine, emphasizing the labile coordination of the imine ligands. Weak imine binding corroborates the low stability of the bimetallic complexes **9** and **10**.

Redox-active organometallic polymers

Combination of the two synthons, *i.e.* the dicarbene bridged bimetallic complexes and the diimine linked systems, allowed

§ A characteristic feature of the ^1H NMR spectrum of **12** is the magnetic inequivalence of the CH_3 protons of the *i*Pr wingtip groups giving rise to two signals at RT (δ_H 1.63 and 0.99 in acetone-d_6). On cooling to –35 °C the signals decoalesce into four magnetically inequivalent resonances. The two signals at lower field coalesce at $T_c = 251(\pm2)$ K, corresponding to an approximate free energy of activation $\Delta G‡ = 51.7(\pm0.5)$ kJ mol^{-1}, while the two signals at higher field show coalescence at $T_c = 278(\pm2)$ K ($\Delta G‡ = 52.4(\pm0.4)$ kJ mol^{-1}). Such dynamic behavior may be rationalized by hindered rotation about the N–C_{iPr} bond. This rotation is expected to be slightly different for the two *i*Pr wingtips because of the unequal steric demand of the CO and pyridine ligands. In addition, line broadening was observed for the *ortho*-H_{py} resonances at low temperature, suggesting that rotation about the Fe–N_{py} bond is slow on the NMR time scale. This result is in good agreement with the broad pyrazine resonances observed for **9a**.

Table 6 Selected bond lengths (Å) and angles (°) for **11** and **12**[a]

	11	**12**
Fe1–C7	1.969(3)	1.972(2)
Fe1–$C_{centroid}$	1.716(2)	1.736(1)
Fe1–C6	1.770(3)	1.750(2)
Fe1–N3	1.915(2)	2.017(1)
C7–N1	1.362(3)	1.363(2)
C7–N2	1.360(3)	1.365(2)
N1–C8	1.381(4)	1.383(2)
N2–C9	1.390(4)	1.389(2)
C8–C9	1.340(4)	1.338(2)
C7–Fe1–N3	93.5(1)	88.69(5)
C7–Fe1–C6	94.3(1)	98.79(7)
C6–Fe1–N3	92.0(1)	90.22(6)
N1–C7–N2	104.2(2)	104.09(12)

[a] Estimated standard deviations in parentheses.

for synthesizing main-chain organometallic co-polymers. Due to the mild conditions required for imine coordination as opposed to carbene bonding, the polymers were prepared starting from synthon **A**, that is, complexes containing the dicarbene ligand already installed at the metal center. Based on the reactivity protocols established for imine coordination to the monometallic precursor **7** and **8** (*viz.* the synthesis of the bimetallic complexes **9** and **10**) the bimetallic complex **5** containing butyl wingtip groups and a rigid phenylene spacer between the carbene units was irradiated in the presence of pyrazine or bipyridine as interlinking diimine ligand. Photochemically induced CO dissociation thus yielded the corresponding polymers **13a** and **14a**, which readily precipitated from the reaction mixture (Scheme 4). The bimetallic complex **3** comprising mesityl wingtip groups required treatment with one mole equivalent of diimine in the presence of two mole equivalents of $AgBF_4$ to afford the analogous polymers **13b** and **14b**.

Formation of oligo- or polymeric products was indicated by spectroscopy and electrochemistry. While ^{1}H NMR spectroscopy showed considerably broadened resonances, the UV-Vis absorption spectra of **13** and **14** are reminiscent to those of complexes **9** and **10** and suggest binding of the diimine ligand to two iron centers. The pyrazine-containing polymers showed two absorption maxima located at around 420 nm and 540 nm (Table 1), which is in excellent agreement with the bimetallic synthon **9** (*cf.* Table 5). The polymers with bipyridine exhibit a single absorption maximum with λ_{max} around 460 nm. Similarly, the single ν_{CO} absorption provided a diagnostic probe, specifically when starting from the dicarbonyl precursor **5**. For **14a**, the strongest absorption was located at ν_{CO} = 1937 cm^{-1}, which corroborates the data for **10a**. When pyrazine was used, however, the presence of the two bands at higher energy (ν = 2043 and 1991 cm^{-1}) along with a band at ν_{CO} = 1969 cm^{-1} suggested that, while the desired polymer was formed, some starting material was not consumed.

Electrochemical analysis using CV also supported polymer formation. The half-wave potentials were similar to those of the bimetallic model complexes and hence indicate the anticipated substitution of a carbonyl or iodide ligand at iron with the corresponding diimine ligand (Table 1). Notably, the *quasi*-reversible redox wave of the pyrazine-containing polymers **13** were unusually broad, and the maximum current I_{max} was relatively low (Fig. 8(a)). Such behavior may be explained either by multiple metal–metal interactions, similar to those observed in the corresponding bimetallic system **9b**, or more likely, by the fact that the electron transfer is not only diffusion-controlled. The latter is expected in polymers because of their limited rotational flexibility as compared to molecular species in solution. The redox process of the bipyridine analog **14b** was considerably sharper, perhaps as a consequence of a low polymerization degree and formation of oligomers only. Indeed, microanalyses of complexes **14** were in line with the presence of tri- and tetramers.¶

Unexpectedly, time-dependent monitoring of the UV-Vis absorption at λ_{max} revealed a substantially better stability of the polymeric systems as opposed to the bimetallic complexes. This effect was particularly pronounced in the pyrazine-containing polymer **13a**. While the half-life time of the bimetallic analog **9a** in $MeNO_2$ was on the order of 30 s, polymer **13a** had $t_{1/2}$ ~ 10 min (Fig. 8(b)). Such increased stability may be useful for processing these polymers, *e.g.* by spin coating. After solvent

¶ The weak imine coordination prevented further analyses such as mass spectrometry or gel permeation chromatography. Only (poly)cationic fragments of the type [(cp)Fe(dicarbene)Fe(cp)] were detectable.

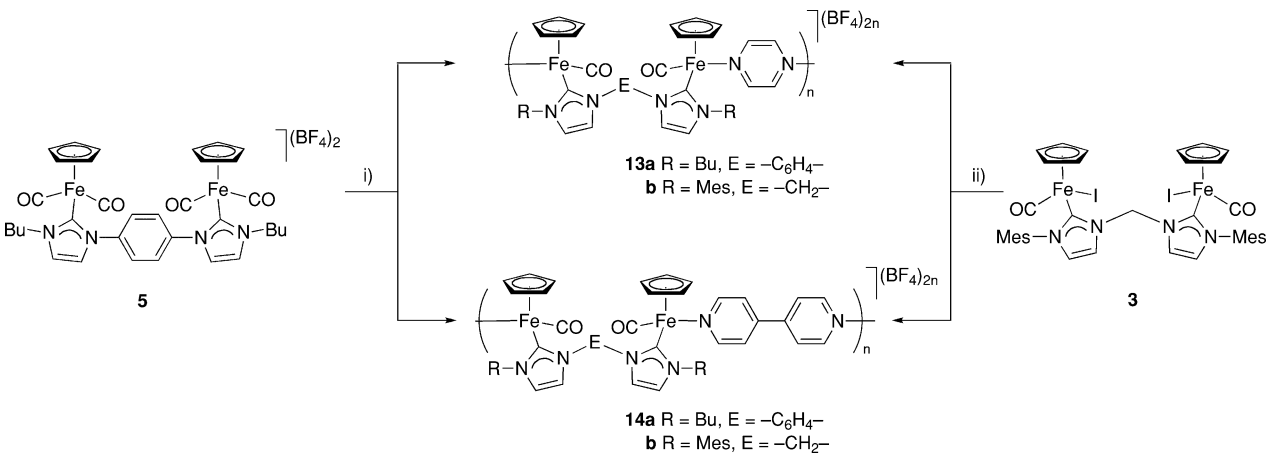

Scheme 4 Synthesis of organometallic co-polymers; reagents and conditions: (i) pyrazine or 4,4′-bipyridine, *hν*, acetone; (ii) pyrazine or 4,4′-bipyridyl, $AgBF_4$, CH_2Cl_2.

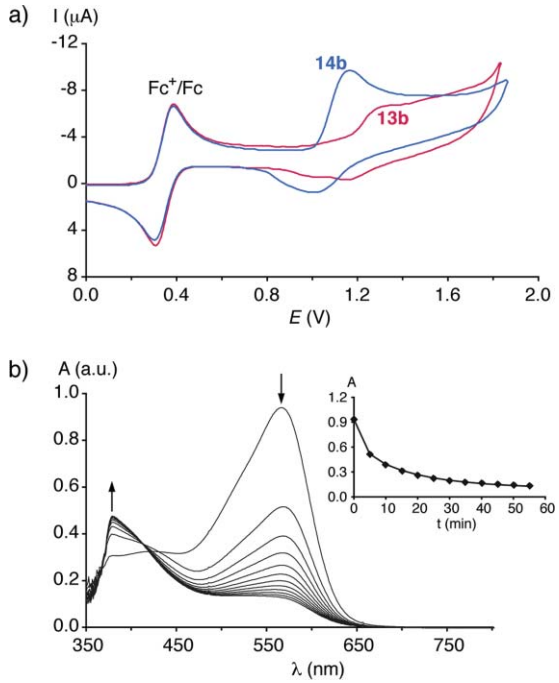

Fig. 8 (a) CV of the pyrazine-containing polymer **13b** and its bipyridine analog **14b** in $MeNO_2$ (100 mV s^{-1} scan rate, Bu_4NPF_6 as supporting electrolyte, glassy carbon working electrode); (b) spectral change of **13a** in $MeNO_2$, at 5 min time intervals; inset shows the time-dependent absorption at 568 nm.

evaporation, the stability increases significantly and in the solid state, no decomposition has been observed thus far.

Conclusions

Organometallic polymers comprised of redox-active metal centers in the polymer main-chain have been synthesized by co-polymerization of bimetallic iron(II) NHC complexes with pyrazine and 4,4′-bipyridine as ditopic diimine ligands. The polymers are redox-active and cyclic voltammetry experiments indicate that the metal centers are electronically coupled when pyrazine was used as interconnecting ligand. The polymers formed are reasonably stable towards air and moisture in the solid state, but they decompose gradually in solution. Comparative studies on analogous bimetallic complexes suggest that the decomposition is due to the dissociation of the weakly coordinating N-donor ligands. In order to use such types of polymers in molecular electronic applications, it will therefore be necessary to increase the stability of the imine bonding, perhaps *via* chelation. Studies in this direction and also towards the full exploitation of the electrochemical properties of the polymers are in progress.

Acknowledgements

We thank Felix Fehr for NMR assistance and the Swiss National Science Foundation for financial support. M. A. gratefully acknowledges an Assistant Professorship of the Alfred Werner Foundation.

Notes and references

1 (*a*) W. A. Herrmann and C. Köcher, *Angew. Chem., Int. Ed.*, 2002, **41**, 1290; (*b*) *N-Heterocyclic Carbenes in Synthesis*, ed. S. P. Nolan, Wiley-VCH, Weinheim, Germany, 2006; (*c*) F. E. Hahn and M. C. Jahnke, *Angew. Chem., Int. Ed.*, 2008, **47**, 3122.
2 (*a*) NHC in biological applications: A. Melaiye, Z. Sun, K. Hindi, A. Milsted, D. Ely, D. H. Reneker, C. A. Tessier and W. J. Youngs, *J. Am. Chem. Soc.*, 2005, **127**, 2285; (*b*) A. Kascatan-Nebioglu, M. J. Panzner, C. A. Tessier, C. L. Cannon and W. J. Youngs, *Coord. Chem. Rev.*, 2007, **251**, 884; (*c*) P. J. Barnard and S. J. Berners-Price, *Coord. Chem. Rev.*, 2007, **251**, 1889; (*d*) P. J. Barnard, R. A. Ruhayel, M. M. Jellicoe, J. L. Hickey, M. V. Baker and S. J. Berners-Price, *J. Am. Chem. Soc.*, 2008, **130**, 12570.
3 (*a*) NHC in photoluminescent applications: T. Sajoto, P. I. Djurovich, A. Tamayo, M. Yousufuddin, R. Bau, M. E. Thompson, R. J. Holmes and S. R. Forrest, *Inorg. Chem.*, 2005, **44**, 7992; (*b*) C.-F. Chang, Y.-M. Cheng, Y. Chi, Y.-C. Chiu, C.-C. Lin, G.-H. Lee, P.-T. Chou, C.-C. Chen, C.-H. Chang and C.-C. Wu, *Angew. Chem., Int. Ed.*, 2008, **47**, 4542; (*c*) Y. Unger, A. Zeller, S. Ahrens and T. Strassner, *Chem. Commun.*, 2008, 3263; (*d*) H. M. J. Wang, C. Y. L. Chen and I. J. B. Lin, *Organometallics*, 1999, **18**, 1216; (*e*) V. J. Catalano, M. A. Malwitz and A. O. Etogo, *Inorg. Chem.*, 2004, **43**, 5714.
4 NHC as gelators: T. Tu, X. Bao, W. Assenmacher, H. Peterlik, J. Daniels and K. H. Dötz, *Chem.–Eur. J.*, 2009, **15**, 1853.
5 (*a*) D. Bourissou, O. Guerret, F. Gabbai and G. Bertrand, *Chem. Rev.*, 2000, **100**, 39; (*b*) W. A. Herrmann, *Angew. Chem., Int. Ed.*, 2002, **41**, 1290; (*c*) M. Lee and C. Hu, *Organometallics*, 2004, **23**, 976.
6 (*a*) D. S. McGuinness, N. Saendig, B. F. Yates and K. J. Cavell, *J. Am. Chem. Soc.*, 2001, **123**, 4029; (*b*) D. Nemcsok, K. Wichmann and G. Frenking, *Organometallics*, 2004, **23**, 3640; (*c*) H. Jacobsen, A. Correa, C. Costabile and L. Cavallo, *J. Organomet. Chem.*, 2006, **691**, 4350; (*d*) L. Gagliardi and C. J. Cramer, *Inorg. Chem.*, 2006, **45**, 9442; (*e*) H. Jacobsen, A. Correa, A. Poater, C. Costabile and L. Cavallo, *Coord. Chem. Rev.*, 2009, **253**, 687.
7 (*a*) A. J. Arduengo, S. F. Gamper, J. C. Calabrese and F. Davidson, *J. Am. Chem. Soc.*, 1994, **116**, 4391; (*b*) A. D. D. Tulloch, A. B. Danopoulos, S. Kleinhenz, M. E. Light, M. B. Hursthouse and G. Eastham, *Organometallics*, 2001, **20**, 2027; (*c*) X. Hu, I. Castro-Rodriguez, K. Olsen and K. Meyer, *Organometallics*, 2004, **23**, 755; (*d*) S. Saravankumar, A. I. Oprea, M. K. Kindermann, P. G. Jones and J. Heinicke, *Chem.–Eur. J.*, 2006, **12**, 3143; (*e*) W. A. Herrmann, J. Schütz, G. D. Frey and E. Herdtweck, *Organometallics*, 2006, **25**, 2437; (*f*) J. C. Green and B. J. Herbert, *Dalton Trans.*, 2005, 1214; (*g*) S. Fantasia, J. L. Petersen, H. Jacobsen, L. Cavallo and S. P. Nolan, *Organometallics*, 2007, **26**, 5880.
8 (*a*) P. Nguyen, P. Gómez-Elipe and I. Manners, *Chem. Rev.*, 1999, **99**, 1515; (*b*) B. J. Holliday and T. M. Swager, *Chem. Commun.*, 2005, 23; (*c*) K. A. Williams, A. J. Boydston and C. W. Bielawski, *Chem. Soc. Rev.*, 2007, **36**, 729.
9 (*a*) O. Guerret, S. Solé, H. Gornitzka, M. Teichert, G. Trinquier and G. Bertrand, *J. Am. Chem. Soc.*, 1997, **119**, 6668; (*b*) V. J. Catalano and A. L. Moore, *Inorg. Chem.*, 2005, **44**, 6558; (*c*) A. J. Boydston, K. A. Williams and C. W. Bielawski, *J. Am. Chem. Soc.*, 2005, **127**, 12496; (*d*) A. J. Boydston, J. D. Rice, M. D. Sanderson, O. L. Dykhno and C. W. Bielawski, *Organometallics*, 2006, **25**, 6087.
10 (*a*) A. J. Boydston and C. W. Bielawski, *Dalton Trans.*, 2006, 4073; (*b*) A. J. Boydston, J. W. Kamplain and C. W. Bielawski, *Chem. Commun.*, 2006, 1727.
11 L. Mercs, A. Neels and M. Albrecht, *Dalton Trans.*, 2008, 5570.
12 F. E. Hahn, C. Radloff, T. Pape and A. Hepp, *Organometallics*, 2008, **27**, 6408.
13 L. Mercs, G. Labat, A. Neels, A. Ehlers and M. Albrecht, *Organometallics*, 2006, **25**, 5648.
14 M. G. Gardiner, W. A. Herrmann, C.-P. Reisinger, J. Schwarz and M. Spiegler, *J. Organomet. Chem.*, 1999, **572**, 239.
15 L. Mercs, A. Neels and M. Albrecht, manuscript in preparation.
16 P. Buchgraber, L. Toupet and V. Guerchais, *Organometallics*, 2003, **22**, 5144.
17 N. G. Connelly and W. E. Geiger, *Chem. Rev.*, 1996, **96**, 877.
18 Determined using ferrocenium/ferrocene as a reference ($E_{1/2} = 0.46$ V *vs.* SCE).
19 G. M. Scheldrick, *Acta Crystallogr., Sect. A: Fundam. Crystallogr.*, 2008, **64**, 112.

20 A. Altomare, G. Cascarano, C. Giacovazzo, A. Guagliardi, M. C. Burla, G. Polidori and M. Camalli, *SIR92, J. Appl. Crystallogr.*, 1994, **27**, 435.
21 R. H. Blessing, *Acta Crystallogr., Sect. A: Fundam. Crystallogr.*, 1995, **51**, 33.
22 A. L. Spek, *Acta Crystallogr., Sect. D: Biol. Crystallogr.*, 2009, **65**, 148.
23 J. Mata, A. R. Chianese, J. R. Miecznikowski, M. Poyatos, E. Peris, J. W. Faller and R. H. Crabtree, *Organometallics*, 2004, **23**, 1253.
24 (*a*) H. G. Raubenheimer, F. Scott, S. Cronje, P. H. Rooyen and K. Psotta, *J. Chem. Soc., Dalton Trans.*, 1992, 1009; (*b*) A. A. Danopoulos, N. Tsoureas, J. A. Wright and M. E. Light, *Organometallics*, 2004, **23**, 166; (*c*) J.-F. Capon, S. El Hassnaoui, F. Gloaguen, P. Schollhammer and J. Talarmin, *Organometallics*, 2005, **24**, 2020.
25 M. B. Robin and P. Day, *Adv. Inorg. Chem. Radiochem.*, 1967, **10**, 247.
26 C. A. Hunter and J. K. M. Sanders, *J. Am. Chem. Soc.*, 1990, **112**, 5525.